Small-angle neutron scattering analysis of the microstructure of Stomaflex Crème - Ferrofluid based elastomers

E. M. ANITAS[a,b*], M. BALASOIU[a,c], I. BICA[b], V. A. OSIPOV[a], A. I. KUKLIN[a]
[a]*Joint Institute for Nuclear Research, 141980 Dubna, Moscow region, Russian Federation*
[b]*The West University of Timisoara, Blvd. V. Parvan, No. 4, 300223 Timisoara, Romania*
[c]*Horia Hulubei National Institute of Physics and Nuclear Engineering, Bucharest, Romania*

The microstructure of Stomaflex Crème (SC) and of magnetic elastomers obtained by the addition of ferrofluid (FF) to the SC polymer matrix has been investigated by small-angle neutron scattering (SANS) within the q-interval $0.006\ \text{Å}^{-1} \leq q \leq 0.6\ \text{Å}^{-1}$. Two kinds of elastomers were analyzed: polymerized with and without magnetic field at 2.2% mass concentration of magnetic particles. SANS data from SC exhibit a $q^{-3.5}$ behavior, while for magnetic elastomers, two power-laws ($q^{-2.3}$ for low q and q^{-4} for high q) and one exponential regime are observed. The fractal dimensions for SC and magnetic elastomers, and radius of gyration of magnetic particles were quantified by approximating SANS data with a surface fractal model and unified exponential/power-law approach, respectively.

(Received May 15, 2009; accepted June 15, 2009)

Keywords: SANS, Magnetic elastomers, Stomaflex crème, Surface fractals, Exponential/power-law approach

1. Introduction

Magnetic elastomers represent a new type of composites, consisting of nano/micro sized magnetic particles dispersed in a polymer matrix. The main advantage of these composites resides in the possibility of combining physical properties of the constituents to obtain new structural or functional properties. Therefore, they are intensively studied [1 - 6] and many scientific efforts are focused on the comprehension and optimization of their structural performances [7, 8]. A precise description of the microscopic structure using only conventional techniques as electron or atomic force microscopy is often difficult to obtain. Small angle scattering techniques [9 - 11] of neutrons or x-rays are proved to be a very powerful tool for investigation of polymers [12, 13]. This is due to the fact that many quantities of interest (i.e. specific surface) can be extracted with almost no approximation or model. Particularly, in magnetic elastomers SANS is very suitable for structural analysis due to interactions between neutrons and atomic nuclei (nuclear scattering), and interactions between magnetic moments of neutrons and magnetic atoms (magnetic scattering). The obtained informations from the SANS curves serves purposes ranging from understanding the way in which particles are distributed in the polymer matrix until the possibility of controlling certain material properties. Thus, together with electron microscopy (EM) technique, they are the primarily tools for description of the microstructure of a SC polymer filled with FF [14] and of primary particles in FF. Such polymers, filled with both micrometer and nano sized magnetic particles are intensively studied [16, 19]. Several determinations of nanometric primary particle sizes for FF from the same producer [15] have been reported earlier in Refs. [17 - 19], using different approaches: core-shell model, modified basic functions and Guinier approximation.

In the present work, mathematical models of surface fractals [20] for SC and unified exponential/power-law [21] for magnetic elastomers are presented and discussed. In addition, spherical form factor together with EM images are used to confirm the magnitude of radius of magnetic particles obtained using the model for magnetic elastomers. Results from SANS experiments showing the characteristic sizes and modifications of scattering intensity with magnetic field used in the polymerization process are presented and analyzed.

2. Experimental and theoretical methods

Two sets of magnetic elastomers samples were produced by addition of FF to a commercially available product SC: polymerized without magnetic field (ME1) and with magnetic field $150.5\ mT$ (ME2). In both cases the mass concentration of magnetic particles is $2.2\ \%$. TEM observations performed on FF show particles with approximately a spherical shape and a radius of about $4.1\ nm$.

SANS measurements were carried out using the YUMO [22, 23] instrument installed at IBR-2 pulsed reactor (JINR, Dubna, Russia), equipped with a two-detector system. Processing of the measured spectrum, calculation of the spectrometer resolution, carrying out the spectrum normalization were performed using SAS software package [24]. The coverage interval of scattering vector q was $0.006\ \text{Å}^{-1} \ll q \ll 0.6\ \text{Å}^{-1}$, where the magnitude $q = |\vec{q}| = |\vec{k} - \vec{k}_0|$ with $\vec{k}$ and $\vec{k}_0$ the wave vectors of incident and scattered neutrons, has the expression:

$$q = \left(\frac{4\pi}{\lambda}\right)\sin\left(\frac{\theta}{2}\right) \tag{1}$$

where λ is the incident neutron wavelength and θ is the scattering angle.

The influence of magnetic particles in ME1 scattering profile was determined by subtracting the contribution of SC from ME1 sample. From this we were able to fit this contribution with a spherical form factor of the form:

$$P(q) = C\frac{(\sin(qr_0) - qr_0\cos(qr_0))^2}{(qr_0)^6} \tag{2}$$

where C is a constant which include particle volume and its scattering length density, and r_0 is sphere radius.

The theoretical description of the whole scattering curves to determine d_f and R_g were made in the framework of surface fractals for SC and the unified exponential/power-law approach for ME1. Surface fractals [25] are objects whose surface area S increases with the radius according to: $S(r) = S_0 r^{d_f}, \quad (d-1 \le d_f < d)$, where S_0 is a positive real number (and d is the Euclidean dimension in which the object is embedded). When $d = 3$, a value of d_f close to two indicate a uniform object while a value close to three an object with extremely rough surfaces. For these objects, the scattered intensity can be approximated by [20]:

$$I(q) = I_0\Gamma(3 - d_f)\sin\left[\frac{\pi(d_f - 1)}{2}\right]q^{-(6-d_f)} + A \tag{3}$$

where, I_0 is a constant that depends on both the experimental conditions and the structure of the fractal, $\Gamma(3 - d_f)$ is the gamma function and A is the background. From eqn. (3) it can be seen that the fractal nature of the structure within a given spatial range is proved by a power-law dependence of $I(q)$ within a given q-interval $(I(q) \sim q^{-\alpha}, \quad \alpha = 6 - d_f)$. The unified exponential/power-law approach is expressed as:

$$I(q) = \sum_{i=1}^{n}\{[G_i \exp(-(q^2 R_{gi}^2)/3) + B_i \exp(-(q^2 R_{g(i+1)}^2)/3)\left[(\operatorname{erf}(qR_{gi}/\sqrt{6}))^3\right]^{P_i}\} \tag{4}$$

where n is the number of structural levels observed, G_i are Guinier prefactors, B_i are prefactors specific to the type of power-law scattering, specified by the regime in which the exponent P falls, and erf is the error function. For surface fractals [26].

$$B_i = 4\pi\rho^2 R_g^{6-P_i}\Gamma\left((P_i - 1)\sin\left(\frac{\pi(P_i - 3)}{2}\right)\right)(P_i - 3)$$

The first term in eqn. (4) describe a large-structure of average size R_{gi} composed of small-scale structures of average size $R_{g(i+1)}$. The second term allows for power-law regimes for the large structure. Every structural level i is described by four parameters G_i, R_{gi}, B_i and P_i.

From equations (3) and (4), fractal dimension d_f of SC, and radius of gyration of magnetic particles R_{gs} and power law exponent P_1 in exponential/power-law approach of magnetic elastomers were obtained.

3. Results

A typical micrograph on FF is presented in Fig. 1 together with the size distribution in Fig. 2 which shows that magnetic particles, with $\langle d \rangle = 8.2$ nm and $\sigma = 2.4$ nm, in a good approximation can be considered to be spherically.

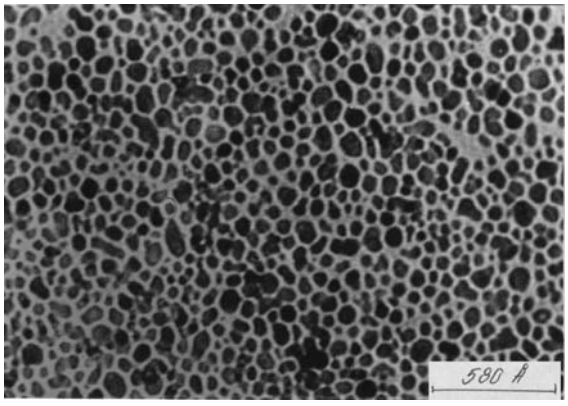

Fig. 1. TEM picture for FF before addition to SC.

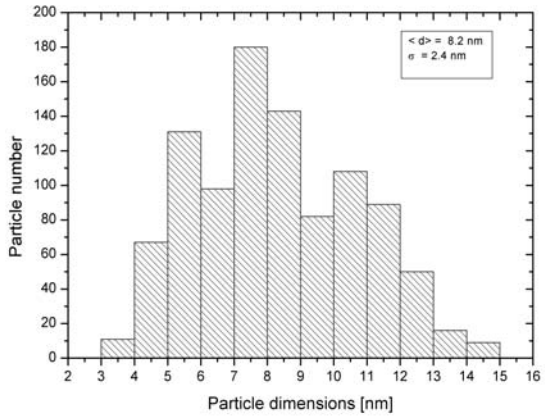

Fig. 2. Size distribution of magnetic particles from electron microscopy images.

Fig. 3 show the SANS scattering intensity vs. the magnitude of the scattering vector q for SC, ME1 and ME2 respectively. For SC the scattering profile show a power law regime at low q values $0.006\ \text{Å}^{-1} \ll q \ll 0.033\ \text{Å}^{-1}$.

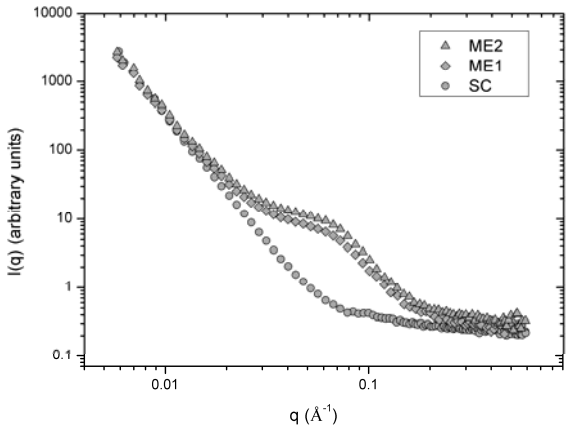

Fig. 3. The SANS experimental data for SC and magnetic elastomers.

Scattering from magnetic particles is obtained by subtraction of SC from ME1, where we see only nuclear scattering (Fig. 4) and a fit with the spherical form factor (eqn. 2) gives a radius for magnetic particles of $3.7\ \text{nm}$.

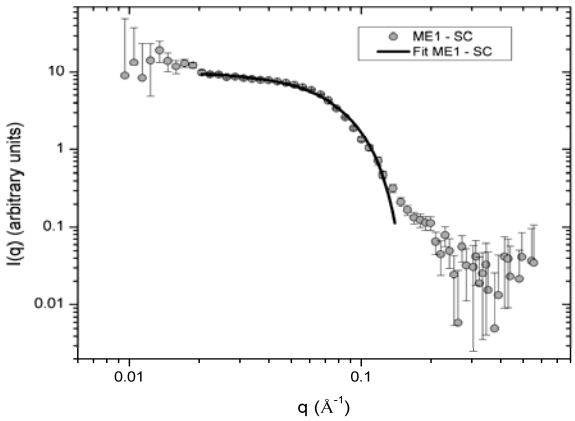

Fig. 4. The SANS experimental data after SC subtraction. Full line is the fit with spherical form factor from eqn. (2).

Further, fitting the experimental data from SC using eqn. (3), a fractal dimension of 2.5 is obtained (Fig. 5) which implies that SC contains networks of rough surfaces in observed q-range.

Applying the unified exponential/power-law approach (eqn. 4) to data from ME1 (Fig. 6) with two structural levels of ME1, the large-scale structure at low q is determined to display surface-fractal scaling. At high q, contribution from magnetic particles limits the surface fractal regime. The high q knee at $q \sim 0.08\ \text{Å}^{-1}$ corresponds to the magnetic particles radii, parameter R_{g2} in eqn. (4). Data have been fitted using eqn. (4) for $n = 2$, fixed parameters $G_1 = 0$ since the low q Guinier is not observed, $P_2 = 4$ since the surface of particles is smooth, and background 0.28. The obtained parameters $P_1 = 3.3$, $R_{g2} = 29\ \text{Å}$ and $R_{g1} > 1000\ \text{Å}$ show informations about the structural changes in ME1. The decrease of parameter P_1, which gives in essence the surface fractal dimension, as discussed above, decrease from 3.5 to 3.3 with a possible interpretation that FF addition to ME1 is followed by an increasing of elastomer surface roughness.

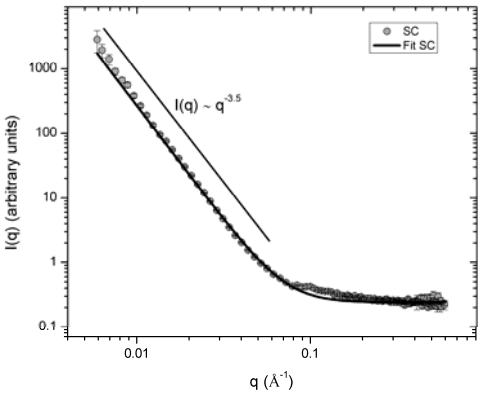

Fig. 5. The SANS experimental data from SC. Full line is the fit using eqn. (3) and a background term.

The value of parameter R_{g1} is at least 1000 Å since the minimum q-value recorded is 0.060 Å^{-1} and in our framework could be connected with the minimum dimension of pores contained in ME1.

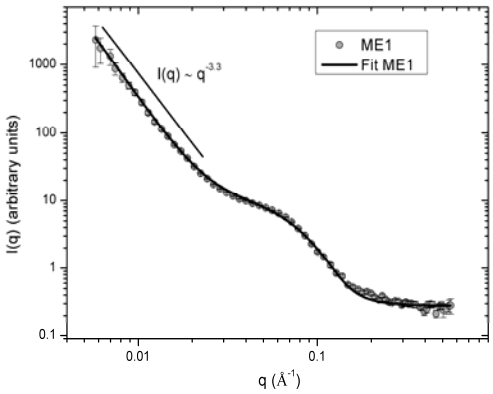

Fig. 6. The SANS experimental data from ME1. The full line is a fit using eqn. (4).

4. Discussion

The results from this study show two essential features of ME1 composites and SC polymer matrix. First, the mean dimension of magnetic particles used in ME1 is about 8.2 nm and their shape is approximately spherical. Second, the structural properties of SC are substantially modified by the addition of FF even at mass concentrations of magnetic particles as low as 2.2 % . For this concentration level, the ME1 composites have a higher roughness than the SC expressed by increasing of the fractal dimension to 2.7 (Fig. 6) from 2.5 (Fig. 5). This roughness increase is attributed to local modifications of SC in the studied q-range where no significant spatial correlations in arrangement of particles themselves or aggregation phenomena are observed. In addition, the mathematical model [20] for SC, and unified exponential/power-law approach [21] for ME1, were found to fit experimental in good agreement with physical significance of parameters. They describe the results obtained and allows us to predict possible structural that are yet unseen, for example the scattering profile of ME1 when the radius of gyration of the first structural level has a given value, bigger than 1000 Å . The use of SANS technique to distinguish features such as magnetic and nuclear scattering has been shown to provide quite small differences between ME1 and ME2. This results from very weak magnetic correlations in the observed q-range, as reported also in [19].

For similar systems the microstructure of SC doped with micrometric Fe particles at different concentrations was reported in Ref. [16]. The radius of magnetic particles used is about $R_0 = 2$ μm , mass concentrations are $25\%, 50\%$ and 75% respectively. Therefore an interaction between particles is observed as a deviation of scattering intensity from the Porod law and from a power-law scattering.

A considerable body of evidence now exists that supports the statement that addition of a FF into a SC, even for low mass concentrations as 2.2% determine a modification of fractal dimension. These modifications can be associated with concentration level, dimensions and with the value of magnetic field in which the magnetic particles are polymerized. Therefore increasing the value of any of these factors will determine the appearance of a threshold for which none of them can be neglected and interparticle correlations have to be taken into account.

5. Conclusions

Using the surface-fractal model for scattering intensities there was shown that Stomaflex creme has a surface-like fractal behavior with fractal dimension 2.5 . With ferrofluid addition this is modified to 2.7, as determined from the value of slope of first structural level in unified exponential/power-law approach.

The results from EM measurements show that magnetic particles in ferrofluid have a mean radius of 4.1 nm while using a spherical form factor in SANS experimental data obtained by subtraction of Stomaflex Creme contribution from magnetic elastomers polymerized without magnetic field intensity curve, a value of 3.7 nm was obtained. These confirm that unified exponential/power-law approach is a good approximation for SANS data from magnetic elastomers polymerized without magnetic field.

Further experiments with different values of magnetization field and concentrations are required.

Acknowledgments

Acknowledgments is made to the Romanian Governmental Representative at JINR. We are extremely grateful for the help which we received from Dr. Marin Lita and Cristina Muresan.

References

[1] G. Filipcsei, I. Csetneki, A. Szilagyi, M. Zrinyi, Adv. Polym. Sci. **206**, 137 (2007).
[2] Y. L. Raikher, V. I. Stepanov, Advances in Chemical Physics **129**, 419 (2004).
[3] G. K. Auernhammer, D. Collin, P Martinoty, J. Chem. Phys. **124**, 204907 (2006).
[4] Z. Varga, G. Filipcsei, M. Zrinyi, Polymer **47**(1), 227 (2006).
[5] M. Barham, D. J. Steigmann, M. McElfresh, R. E.

Rudd, Smart. Mater. Struct. **17**(5), 055003 (2008).
[6] R. Fuhrer, E. K. Athanassiou, N. A. Luechinger, W. J. Stark, Small **5**(3), 383 (2009).
[7] L. Chen, X. L. Gong, W. H. Li, Smart. Mater. Struct. **16**(6), 2645 (2007).
[8] A. Boczkowska, S. Awietjan, R. Wroblewski, Smart. Mater. Struct. **16**(5), 1924 (2007).
[9] A. Guinier, G. Fournet, Small-Angle Scattering of X-Rays, NY: John Wiley&Sons, 1st ed., 1955.
[10] O. Glatter, O. Kratky, Small angle x-ray scattering, Academic Press, 1982.
[11] L. A. Feigin, D. I. Svergun, Structure Analysis by Small Angle X-Ray and Neutron Scattering, Plenum Press, 1987
[12] J. Higgins, H. C. Benoit, Polymers and Neutron Scattering, Oxford University Press, 1997.
[13] N. Stribeck, B. Smarsly, Scattering Methods and the Properties of Polymer Materials, Springer, 1st ed., 2005.
[14] D. Bica, Rom. Rep. Phys. **47**, 265 (1995).
[15] D. Bica, RO Patent 90078, 1985.
[16] M. Balasoiu, E. M. Anitas, I. Bica, R. Erhan, V. A. Osipov, O. L. Orelovich, D. Savu, S. Savu, A. I. Kuklin, Optoelectron. Adv. Mater. – Rapid Comm. **2**(11), 730 (2008).
[17] M. Balasoiu, M. V. Avdeev, A. I. Kuklin, V. L. Aksenov, D. Hasegan, V. Garamus, A. Schreyer, D. Bica, L. Vekas, V. Almasan, Rom. Rep. Phys. **58**(3), 305 (2006).
[18] M. Balasoiu, M. V. Avdeev, V. L. Aksenov, D. Hasegan, V. M. Garamus, A. Schreyer, D. Bica, L. Vekas, J. Magn. Magn. Mat. **300**(1), e225 (2006).
[19] M. Balasoiu, M. L. Craus, A. I. Kuklin, J. Plestil, V. Haramus, A. Kh. Islamov, R. Erhan, E. M. Anitas, M. Lozovan, V. Tripadus, C. Petrescu, D. Savu, S. Savu, I. Bica, J. Optoelectron. Adv. Mater. **10**(11), 2932 (2008).
[20] H. D. Bale, P. W. Schmidt, Phys. Rev. Lett. **53**, 596 (1984).
[21] G. Beaucage, J. Appl. Cryst. **28**, 717 (1995).
[22] A. I. Kuklin, A. Kh. Islamov, Y. S. Kovalev, P. K. Utrobin, V. I. Gordelyi, Surface **6**, 74 (2006).
[23] A. I. Kuklin, A. Kh. Islamov, V. I. Gordelyi, Neutron News, **16**(3), 16 (2005).
[24] A. G. Soloviev, T. M. Solovieva, A. V. Stadnik, A. Kh. Islamov, A. I. Kuklin, JINR preprint, **P10**-2003-86.
[25] D. Avnir, D. Farin, Nature **308**, 261 (1984).
[26] G. Beaucage, D. W. Schaefer, J. Non-Cryst. Solids **172-174**, 797 (1994).

* Corresponding author: eanitasro@yahoo.com